E&G Quaternary Science Journal
Volume 65 / Number 2 / 2016 / 145-155 / DOI 10.3285/eg.65.2.03
www.quaternary-science.net

GEOZON SCIENCE MEDIA
ISSN 0424-7116

First ^{36}Cl exposure ages from a moraine in the Northern Calcareous Alps

Andrew P. Moran, Susan Ivy-Ochs, Christof Vockenhuber, Hanns Kerschner

How to cite: Moran, A.P., Ivy-Ochs, S., Vockenhuber, Ch. & Kerschner, H. (2016): First ^{36}Cl exposure ages from a moraine in the Northern Calcareous Alps. – E&G Quaternary Science Journal, 65 (2): 145–155. DOI: 10.3285/eg.65.2.03

Abstract: A well-preserved moraine system in the Mieminger Range (Northern Calcareous Alps of Austria) provides geomorphological evidence of a former glacier advance reaching significantly beyond the extent of subsequent glaciation during the "Little Ice Age". The reconstructed palaeoglacier is associated with an equilibrium line altitude lowering of -70 – -120 m and boulders on its moraine were ^{36}Cl dated to the early Holocene (~10.4 ka). Hence, the glacier advance was likely triggered during a phase of glacier-friendly climate within the Preboreal period. On the proximal side of the moraine, further boulders were dated on hummocky moraines within the former glacier tongue area showing considerably younger ages of around 9 ka. In connection with several relict rock glaciers in the cirque that formed subsequently to the glacier advance, these ages point to a prolonged phase of instable conditions, possibly as a consequence of the formation of discontinuous permafrost and periglacial activity within the cirque. All these landforms lie significantly up valley from a series of lateral moraine segments related to the "Egesen" stadial (Younger Dryas cold phase). The ^{36}Cl ages presented here are the first exposure ages gained from moraines in the northern Alps and form a first step for a numerically dated moraine chronology in the northern Alps.

Erste ^{36}Cl Expositionsalter von einer Moräne in den Nördlichen Kalkalpen

Kurzfassung: Ein gut erhaltenes Moränensystem in der Mieminger Kette (österreichische nördliche Kalkalpen) stellt einen geomorphologischen Nachweis eines vergangenen Gletschervorstoßes dar, der deutlich weiter reichte als die spätere Vergletscherung der „Kleinen Eiszeit". Der rekonstruierte Paläogletscher lässt auf eine Erniedrigung der Gleichgewichtslinie von -70 bis -120 m schließen, während Blöcke auf der Moräne mit ^{36}Cl auf das frühe Holozän (~10,4 ka) datiert wurden. Somit erfolgte der Gletschervorstoß höchstwahrscheinlich in einer gletscherfreundlichen Klimaphase während des Präboreals. Auf der inneren Seite der Moräne, im Bereich der ehemaligen Gletscherzunge, wurden weitere Blöcke auf hügeligem Moränenmaterial datiert, die wesentlich jüngere Alter um ungefähr 9 ka aufweisen. In Verbindung mit mehreren fossilen Blockgletschern im Kar, die sich nach dem Gletschervorstoß bildeten, deuten diese Alter auf eine längere Phase instabiler Bedingungen hin. Diese ist möglicherweise durch die Bildung von diskontinuierlichem Permafrost und periglaziale Prozesse im Kar zu erklären. All jene Formen liegen deutlich oberhalb einer Abfolge von Ufermoränensegmenten, die in Verbindung mit dem „Egesenstadial" (Jüngere Dryas Kaltphase) stehen. Die ^{36}Cl Alter, die hier vorgestellt werden, sind die ersten Expositionsalter von einer Moräne in den Nordalpen und bilden einen ersten Baustein für die Erarbeitung einer numerisch datierten Moränenchronologie für diese Alpenregion.

Keywords: *Early Holocene, ^{36}Cl, Glaciers, Palaeoclimate, Exposure dating, Northern Alps, Austria*

Addresses of authors: **Andrew P. Moran***, **Hanns Kerschner**, Institute of Geography, University of Innsbruck, Innrain 52, 6020 Innsbruck, Austria; **Susan Ivy-Ochs, Christof Vockenhuber,** Laboratory of Ion Beam Physics, ETH Zurich, Otto-Stern-Weg 5, 8093 Zurich, Switzerland. **corresponding author: andrew.moran@uibk.ac.at*

1 Introduction

Glaciers react directly to fluctuations in climate through changes in their mass balance. Therefore, where evidence of former glacier extents is found, valuable information on past climate conditions can be derived. In the Alpine region research on glacier-based climate history has been conducted for over a century since Penck & Brückner (1901–1909) resulting in the development of a detailed moraine sequence for the central Alps (Maisch 1981, Ivy-Ochs et al. 2008). In recent decades focus has been placed on the numerical dating of individual Lateglacial and Holocene stadials within the relative moraine sequence to obtain an absolute chronology (Ivy-Ochs et al. 2008, and references therein). Thereby, surface exposure dating with cosmogenic nuclides has emerged as a standard dating tool (Lal 1991, Zreda et al. 1994, Stone 2000, Dunai 2010). It was especially applied in many areas of the Alps to date former glacier advances allocated to the multi-phased "Egesen" stadial (Maisch 1981, Ivy-Ochs et al. 2009, and references therein), which is associated with the Younger Dryas cold period (~12.9 to 11.7 ka; Rasmussen et al. 2006, Ivy-Ochs et al. 2008). However, up valley from these moraines, but yet distinctly beyond Little Ice Age glacier posi-

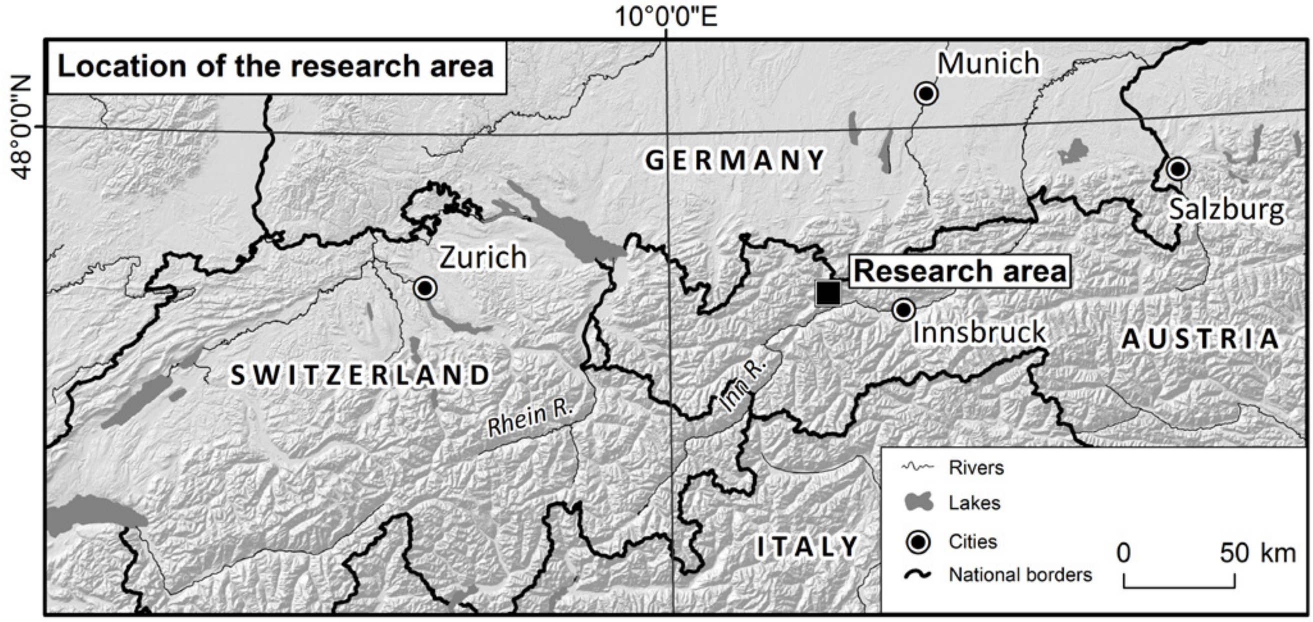

Fig. 1: Location of the research area within the Alpine region.

Abb. 1: Lage des Untersuchungsgebietes im Alpenraum.

tions (maximum extents ~A.D.1850; Maisch 2000) further moraine systems were identified and dated in several areas. Exposure ages relate these glacier advances to the early Holocene period. They infer periods of glacier advances ~10.1 to 10.6 ka (Schindelwig et al. 2011, Schimmelpfennig et al. 2014, Moran, Kerschner & Ivy-Ochs 2015) as well as between ~11.0 and 11.4 ka (Schimmelpfennig et al. 2012, Schimmelpfennig et al. 2014, Moran et al. 2016). The latter may possibly coincide with the multi-centennial cooling phase of the Preboreal Oscillation (~11.4 ka; Björck et al. 1997, Rasmussen et al. 2006). On the other hand, an early Holocene glacier advance is ruled out in the eastern part of the central Alps (Bichler et al. 2016).

While all dated sites are located in the central, southern or western Alps (e.g. Kelly et al. 2004, Ivy-Ochs et al. 2009, Federici et al. 2008, Cossart et al. 2012, Bichler et al. 2016 among others), hitherto no exposure ages have been obtained to determine the timing of glacier advances along the northern Alpine fringe. Therefore we expanded investigations to the Northern Alps, focussing on the region east of Lake Constance, which is particularly interesting because of the high amount of precipitation (Frei & Schmidli 2006) and a topography, characterized by summit heights around 2300–2900 m and an abundance of lower lying cirques with floors around 2000 m a.s.l. where small glaciers could respond more rapidly to short climate fluctuations (Jóhannesson, Raymond & Waddington 1989) than the large glacier systems of the higher central Alps. So far in the Northern Alps, local series of moraines were only defined on the basis of equilibrium line altitudes (ELAs) and their lowerings (ΔELAs) in reference to modern times, as well as on their geomorphological properties (e.g. Keller 1988, Hirtlreiter 1992, Schoeneich 1998). The correlation of the moraines to stadials in the central Alps was primarily based on assumptions of ΔELA gradients within the Alpine region, which may however have varied over time. Furthermore, spatial differences in glacier advance series may be a source of uncertainty in the relative correlation. Therefore, it is expedient to expand numerical dating to the northern Alpine region. Hence, this paper provides first ^{36}Cl ages from a past glacier advance in the Northern Calcareous Alps, forming a preliminary basis for the development of a future northern Alpine moraine chronology based on absolute ages.

2 Research site

Our study area is located in the Mieminger Range of the Northern Calcareous Alps (Figure 1). The mountain chain is about 20 km long and trends from east to west with an average width of around 6 km. It is separated from the higher Wetterstein Mountains by the Gaistal valley in the North and borders on the Mieming Plateau to the South. It extends in the West to the Fernpass and to the Seefeld-Leutasch plateau in the East. The Mieminger Range is exposed to moist, northwesterly air masses from the Atlantic region resulting in high mean annual precipitation sums (~2300 mm/a; Geographie Innsbruck 2013) especially in its northwestern parts. Mesozoic limestone dominates the entire range with Wetterstein limestone accounting for nearly all peaks and exposed bedrock surfaces. Only small parts disclose Middle Triassic Muschelkalk and carbonates of the Reichenhall and Partnach formations (Miller 1962, Becke 1983).

We conducted our investigations in the small, north-facing Schwärzkar cirque in the western part of the mountain range (Figures 2 & 3). The highest peak along the cirque rim is Grünstein, reaching an altitude of 2661 m a.s.l. The foot of the surrounding cirque headwalls consists mainly of fine-grained talus slopes while the floor of the Schwärzkar is mainly covered by glacier transported material and diamicton, containing a series of glacial and periglacial landforms first identified and mapped by Senarclens-Grancy (1938). Denoting the extent of a former glacier in the Schwärzkar, a well-preserved ~700 m long, tongue-shaped moraine ridge extends down to an elevation of ~1950 m a.s.l. near the outlet of the cirque. Its crest is ~5 m above the surrounding

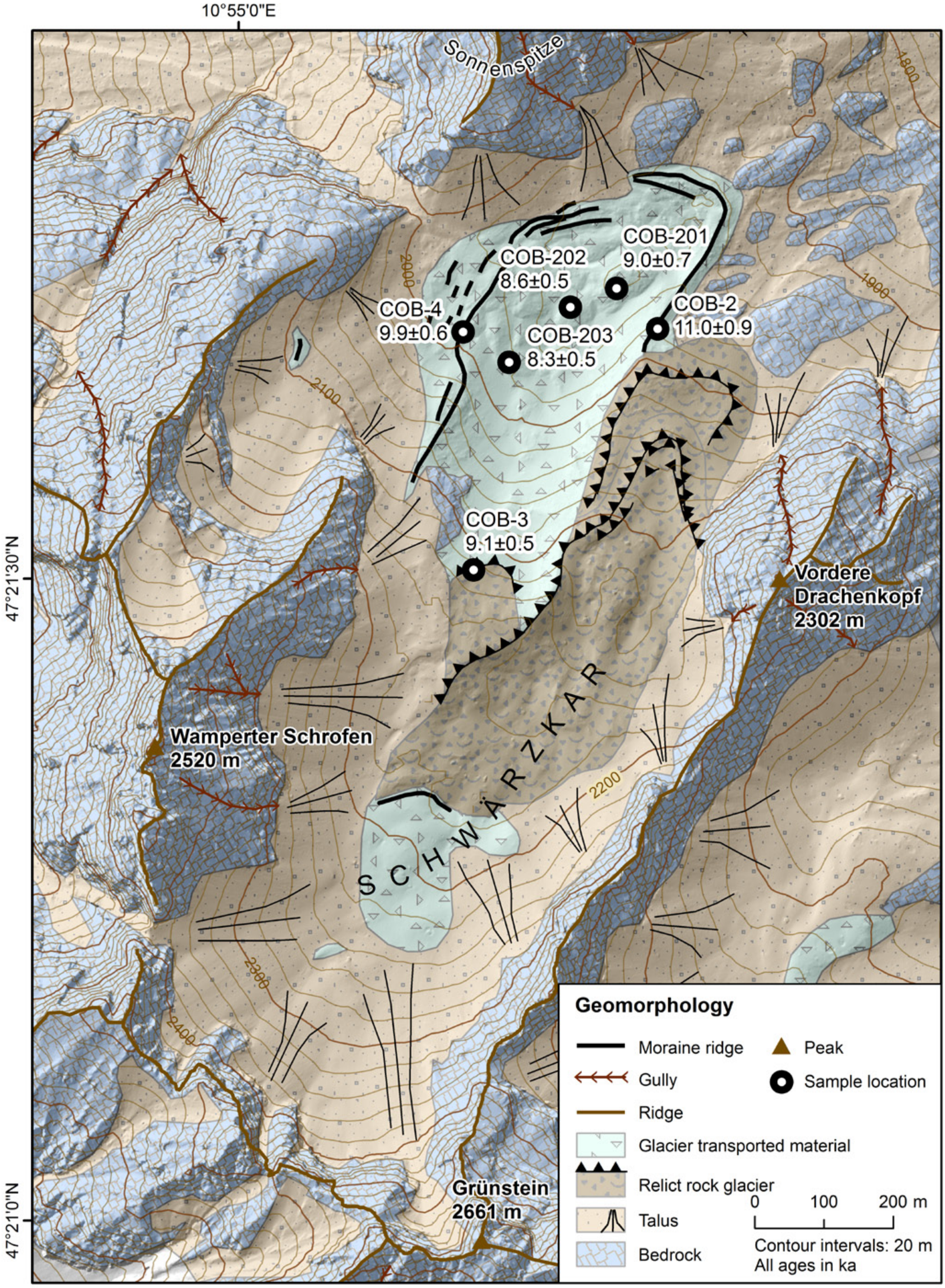

Fig. 2: Geomorphology of the Schwärzkar cirque (Mieminger Range). Source of the Digital Terrain Model: TIRIS Map Service of the Federal State of Tyrol.

Abb. 2: Geomorphologie des Schwärzkars (Mieminger Kette). Quelle des Digitalen Geländemodelles: TIRIS Kartendienst des Landes Tirol.

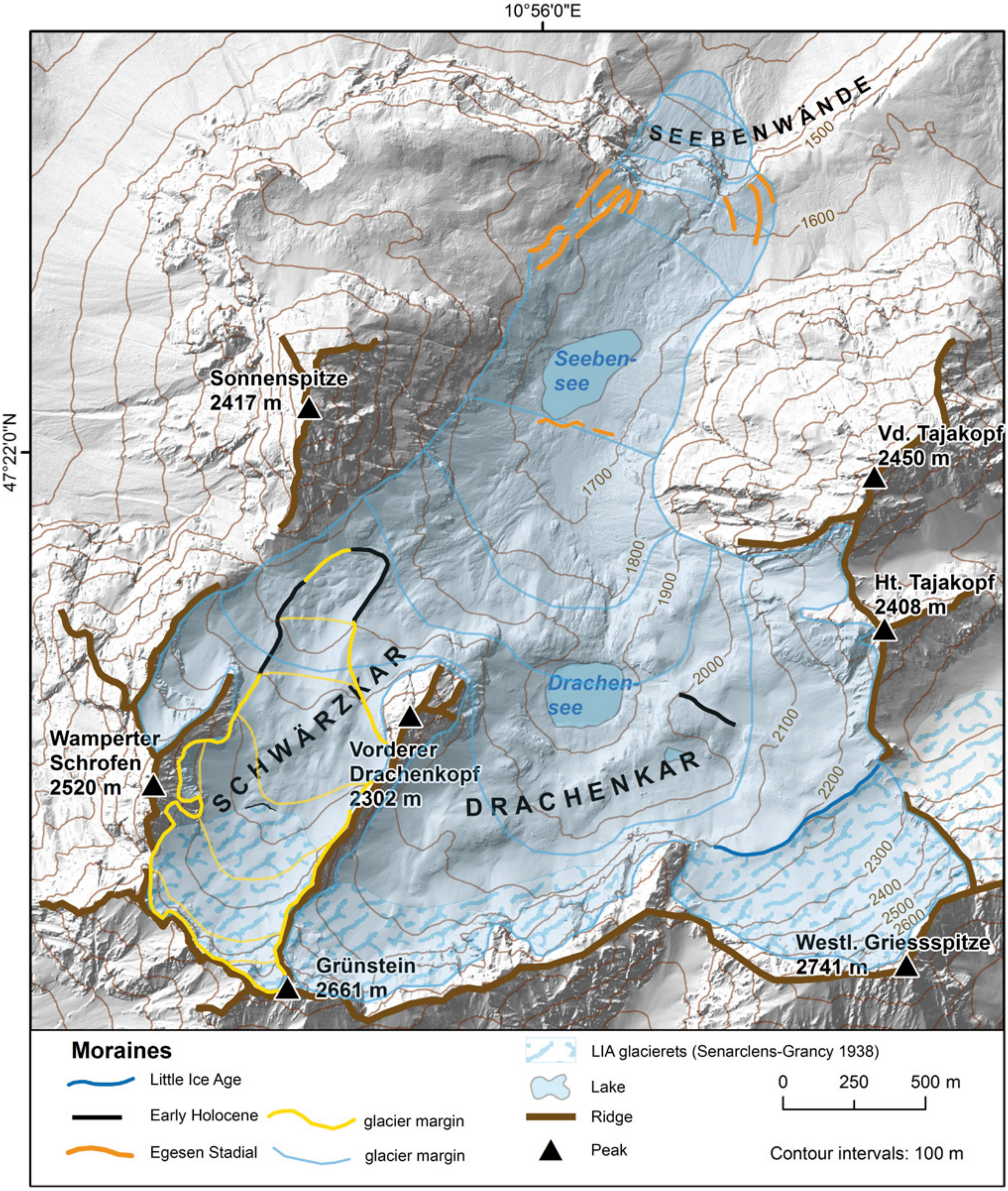

Fig. 3: Outlines of the glaciers in Schwärzkar cirque. For clarity, contour lines of the "Egesen" glacier are only drawn up to 2100 m. "Egesen" moraines in the lower part of the cirque are part of the "younger stadials group" by Senarclens-Grancy (1938). Glacier tongue below 1500 m is hypothetical. Source of the Digital Terrain Model: TIRIS Map Service of the Federal State of Tyrol.

Abb. 3: Umrißlinien und geometrische Eigenschaften der rekonstruierten Gletscher im Schwärzkar. Wegen der Übersichtlichkeit sind die Höhenlinien des Egesengletschers nur bis 2100 m Seehöhe gezeichnet. Die Egesenmoränen sind Teil der „jungstadialen Gruppe" von Senarclens-Grancy (1938). Die Gletscherzunge unterhalb von 1500 m ist hypothetisch. Quelle des Digitalen Geländemodelles: TIRIS Kartendienst des Landes Tirol.

setting at its terminus and its morphologically fresh lateral moraines exhibit steep embankments reaching heights of ~25 m on the eastern side. The western lateral moraine traces the former glacier margin over a distance of ~300 m as a continuous, curved ridge. On its distal side there is a series of subparallel ridges wedged closely against one another. On the proximal side of the lateral moraines, within the lower and flat former glacier tongue area, the surface is marked by boulder fields and block-rich hummocky ridges. They are characterized by a strongly undulated surface with mounds of angular to subangular glacial debris representing positive landforms of ~20 to 40 m in diameter, ris-

E&G / Vol. 65 / No. 2 / 2016 / 145–155 / DOI 10.3285/eg.65.2.03 / © Authors / Creative Commons Attribution License

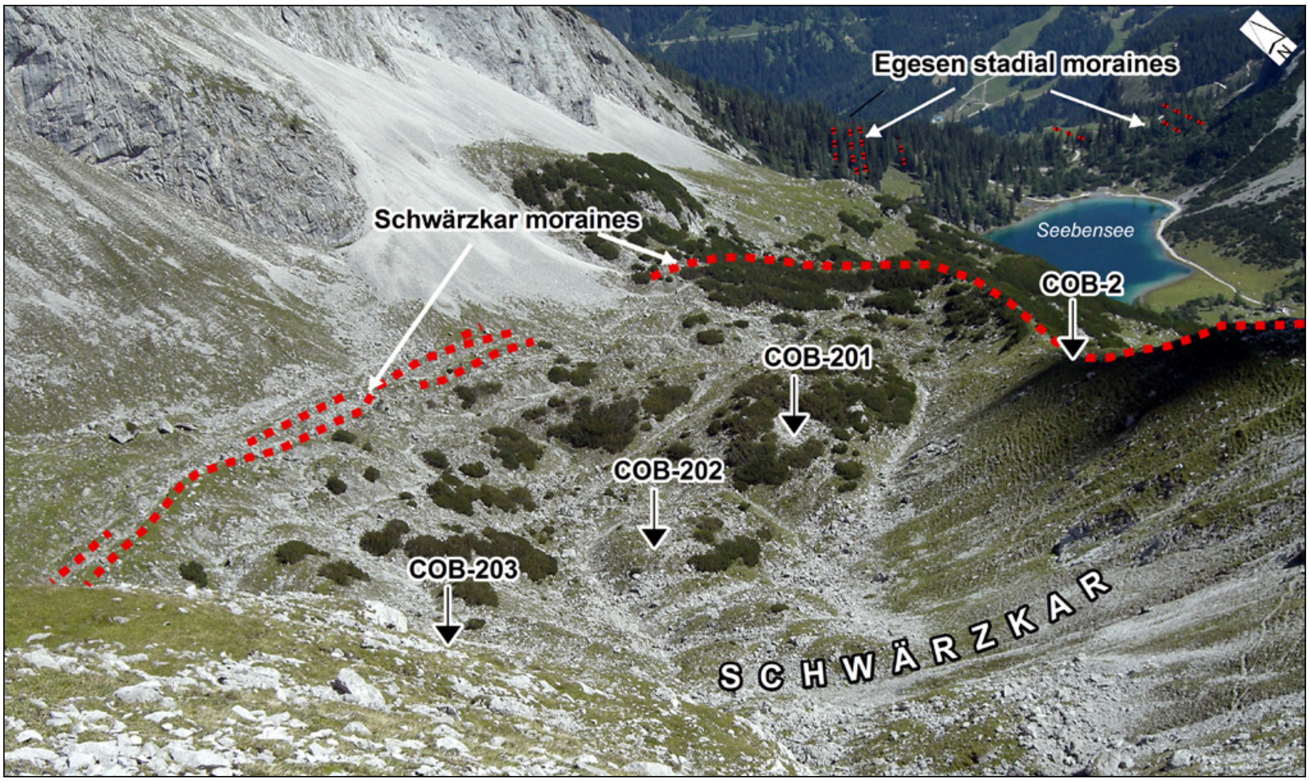

Fig. 4: Photo of the former glacier tongue area of the Schwärzkar palaeoglacier. Sample locations are shown where visible, position of COB-4 is concealed. In the background the lateral moraines of the Egesen stadial are indicated. Photo: A. Moran 2013.

Abb. 4: Foto des ehemaligen Gletscherzungenbereichs des Schwärzkar Paläogletschers. Die Positionen der Probenpunkte werden gezeigt dort wo sie sichtbar sind, COB-4 ist verdeckt. Im Hintergrund sind die Ufermoränen des Egesenstadials angedeutet. Foto: A. Moran 2013.

ing ~10 m above the adjacent surface (Figure 4). The ridges in the frontal part may be interpreted as postdepositional rock glacier movement of glacially transported debris during and after the melt-down of the glacier.

Upvalley from this moraine system, three relict rock glaciers are recognized (Figure 2). The two eastermost exhibit steep outer embankments reaching heights of up to ~20 to 30 m above the surrounding setting with numerous concentric ridges and a surface made up of angular debris. In their upper part an elongated concave structure points to high ice contents during their active phase,and indicating that they may have contained some buried glacier ice (Berthling 2011) in the sense of a glacier-rock glacier continuum (Giardino & Vitek 1988). They lay discordantly over the eastern lateral moraine above an elevation of ~2000 m a.s.l. Large surface boulders within these features are predominantly associated with rock fall from the rock walls of the Vordere Drachenkopf (2302 m a.s.l.; Figure 2). These features are characterized by a series of ridges and a strongly undulated surface in unconsolidated material reflecting one or multiple periods of periglacial creep movement. A third small relict rock glacier lobe ~150 m long and ~110 m wide is found in a central position within the cirque at an elevation of 2160 to 2100 m a.s.l. (Figure 2). Its proximal side is filled with unconsolidated material, while its distal part shows a short but steep embankment. It likely formed from a moraine that was strongly overprinted under periglacial conditions. All these rock glaciers are constrained above by an inconspicuous morainic ridge associated by Senarclens-Grancy (1938) with the Little Ice Age (Figures 2 and 3). According to him the well-shaded upper cirque area was glaciated during modern times. Even today, perennial snow fields are still found directly below the cirque headwalls.. In total, the sequence in the Schwärzkar cirque may be interpreted as an advance of a partly debris covered glacier, which was followed by a period of ice decay and the development of rock glaciers, mainly from formerly glacier-transported material.

Senarclens-Grancy (1938) also mapped moraine segments farther down valley from the Schwärzkar (Figure 3). A series of left and right-hand lateral moraines are found north of Seebensee extending to the edge of the ~250 m high break-off of the Seebenwände above the Ehrwald basin, which he attributed to his "younger stadial group". They trace the glacier margins of a former large oscillating glacier that had its end position in an area of steep rock walls where it presumably formed an impressive ice fall, and whose accumulation area comprised the entire Schwärzkar and neighbouring Drachenkar cirques.

3 Methods

3.1 Dating with cosmogenic radionuclide ^{36}Cl

The stabilization age of the moraine system was determined with the surface exposure dating method (Lal 1991, Stone 2000) for which six boulders on the crest of the moraine or on the proximal side thereof were sampled (Figure 2). The sampling strategy was carried out in accordance with Ivy-Ochs & Kober (2008). Among others, care was taken to select large and stable boulders, whereas surfaces showing karst weathering were preferred over fresh surfaces to exclude sampling surfaces only recently exposed to the atmosphere through

Tab. 1: Major and trace elements of the rock samples (SGS S.A., Canada).

Tab. 1: Haupt- und Spurenelemente der Gesteinsproben (SGS S.A., Kanada).

Sample No.	Al_2O_3	CaO	Cr_2O_3	Fe_2O_3	K_2O	MgO	MnO	Na_2O	P_2O_5	SiO_2	TiO_2	B	Gd	Sm	U	Th
COB-2	0.26	54.20	0	0.11	0	0.50	0.01	0	0.02	1.01	0	<0.01	<0.01	<0.01	<0.01	<0.01
COB-3	0.30	53.60	0	0.16	0	0.53	0.01	0	0	0.98	0	<0.01	<0.01	<0.01	<0.01	<0.01
COB-4	0.64	54.20	0	0.20	0.12	0.86	0.01	0	0.01	1.80	0	<0.01	<0.01	<0.01	<0.01	<0.01
COB-201	0.38	54.90	0	0.09	0.12	0.51	0.01	0	0.02	1.22	0	<0.01	<0.01	<0.01	<0.01	<0.01
COB-202	0.30	54.20	0	0.09	0	0.43	<0.01	0	0	0.81	0	<0.01	<0.01	<0.01	<0.01	<0.01
COB-203	0.36	54.40	0	0.14	0	0.55	0.01	0	0	1.07	0	<0.01	<0.01	<0.01	<0.01	<0.01

spalling. The samples were extracted sufficiently above the surrounding surface to reduce the possibility of exhumation. To avoid selecting boulders deposited by rock fall, we stayed away from the northern left lateral moraines below the Sonnenspitze peak (2417 m a.s.l.; Figure 2). No suitable boulders for sampling were found directly on the crest of the end moraine. Therefore, we sampled two boulders on the crest of the lateral moraines. COB-2 stems from the right lateral moraine, ~220 m from the former glacier terminus and COB-4 from the crest of the left lateral moraine ~400 m from the maximum glacier position. Three further samples (COB-201, COB-202 and COB-203) were collected from large boulders on the proximal side of the former glacier margin on the surface of the hummocky moraines. A final sample (COB-3) stems from a position nearly 200 m higher than the others. This boulder is situated on a small relict rock glacier in the transitional area from the flat upper cirque floor to the lower former tongue area (Figure 2).

From each sample about 60 g of crushed and leached rock with a grain size less than 0.5 mm was prepared for AMS measurements at the Laboratory of Ion Beam Physics, ETH Zurich in compliance with standard laboratory methods (Zreda et al. 1994, Stone et al. 1996, Ivy-Ochs et al. 2004). The $^{36}Cl/Cl$ ratios were measured with the 6 MV tandem accelerator at ETH Zurich relative to the internal standard K382/4N (Christl et al. 2013). Major and trace elements were determined at SGS S.A. (Canada) (Table 1). The ages were calculated with an ETH in-house ^{36}Cl age calculator which implements the equations given in Alfimov & Ivy-Ochs (2009 and references therein). The applied nuclide production rate through spallation of Ca was 48.8±3.4 atoms/g/a and 5.3±1.0 atoms/g/a through muon capture (Stone et al. 1996), while a neutron flux of 760±150 neutrons/g air/a was used for neutron capture reactions (Alfimov & Ivy-Ochs 2009). Production rates were scaled in accordance to Stone (2000). Shielding by the surrounding topography was calculated with the CRONUS Earth online calculator (Balco et al. 2008).

3.2 Palaeoglacier reconstruction and ELA calculations

The reconstruction of the palaeoglacier was conducted based on Carr, Lukas & Mills (2010) and Kirkbride et al. (2015) under consideration of a shear stress of ~100 kPa. The upper glacier margin coincided with the cirque walls while the former glacier tongue could be clearly delimited by the end

*Tab. 2: Exposure ages *including topographic shielding, **including topographic shielding and surface erosion (10 mm/ka). The shielding correction includes topographical shielding, dip and strike of the various boulder surfaces. The uncertainties represent the 1σ confidence interval and comprise AMS counting errors and errors based on the normalization to blanks and standards. All ages are in years before sample extraction (i.e. 2015 AD).*

*Tab. 2: Expositionsalter *inklusive topographische Abschattung, **inklusive topographische Abschattung und Oberflächenerosion (10 mm/ka). Die Abschattungskorrektur beinhaltet die topographische Abschattung sowie das Einfallen und Streichen der jeweiligen Blockoberflächen. Das 1σ Konfidenzintervall schließt alle Unsicherheiten, die aus den AMS Messfehlern stammen, sowie Fehler durch die Abgleichung der Blanks mit den Standards mit ein. Alle Alter sind in Jahre vor der Probenentnahme angegeben (i.e. 2015 n. Chr.).*

Sample No.	Lat. (DD)	Long. (DD)	Altitude (m)	Sample thickness (cm)	Shielding	^{36}Cl atoms $* 10^6 * g^{-1}$	Cl (ppm)	Exposure age* (ka) without erosion correction	Exposure age with erosion correction** (ka)
COB-2	47.360	10.924	1981	1.5	0.893	1.1740±0.0788	80.00±3.36	11.06±0.85	10.95±0.89
COB-3	47.357	10.920	2125	1.5	0.925	1.0829±0.0401	69.86±1.05	9.16±0.47	9.08±0.51
COB-4	47.360	10.920	1995	1.5	0.954	1.0945±0.0508	62.74±1.53	9.84±0.57	9.88±0.61
COB-201	47.361	10.923	1956	1	0.952	1.0411±0.0598	78.12±2.68	9.19±0.63	9.04±0.66
COB-202	47.361	10.922	1952	1	0.944	0.8732±0.0313	38.60±0.54	8.64±0.42	8.85±0.45
COB-203	47.360	10.921	1985	1	0.945	0.9379±0.0313	76.31±1.28	8.32±0.44	8.24±0.48

and lateral moraines. Surface contour lines were drawn at intervals of 50 m. Steady-state ELAs were determined with the accumulation area ratio (AAR) of 0.67, which has yielded reasonable results throughout the Alpine region (Gross, Kerschner & Patzelt 1977, Maisch 1999).

4 Results
4.1 Exposure ages

All obtained cosmogenic ^{36}Cl ages are shown in Table 2. They are presented both with and without an erosion correction of 10 mm/ka, whereas ages with erosion correction form the basis of all further discussions. As the depth profile of ^{36}Cl production within the rock increases for the first decimetres (Ivy-Ochs & Schaller 2009) the consideration of an erosion factor for age calculation can lead to slightly younger ages. The use of somewhat lower (5 mm/ka; Reber et al. 2014) or higher (15 mm/ka; André 2002) erosion rates does not significantly change the results. The uncertainty encompasses the 1σ confidence interval and uncertainties in the production rate. Sample ages are spread widely throughout the early Holocene ranging from 11.0±0.9 ka to 8.2±0.5 ka. While the two oldest ages (11.0±0.9; COB-2 and 9.9±0.6; COB-4) stem from boulders located directly on the lateral moraine crest, all younger ages represent boulder positions on the proximal side of the moraine, clearly within the former glacier tongue area. Further implications of their spatial distribution are discussed below.

Tab. 3: Geographic and geometric properties of the reconstructed Schwärzkar cirque palaeoglacier.

Tab. 3: Geographische und geometrische Eigenschaften des rekonstruierten Schwärzkar Paläogletschers.

Palaeoglacier properties	Results
Area	0.7 km²
Highest point	2550 m a.s.l.
Lowest point	1940 m a.s.l.
Length	1500 m
Aspect	N
ELA	2170 m a.s.l.
ΔELA	-120 m

4.2 Equilibrium line altitudes

The reconstructed surface of the small Schwärzkar palaeoglacier has an area of 0.7 km² and exhibits an ELA of 2170 m a.s.l. (Table 3). Similar ELAs were determined within the Mieminger Range for other cirques. Under the (realistic) assumption of a partial debris cover on the glacier surface, equilibrium conditions may have been maintained with an AAR of 0.5 or less, with an ELA around 2200 to 2220 m.

Based on geomorphological evidence and glacial-geological maps of Senarclens-Grancy (1938), small glacierets existed during the LIA in north-facing, well-shaded cirques (Figure 3). Their ELAs ranged around 2290 m a.s.l. and serve as reference altitudes for the ΔELA calculations.

5 Discussion
5.1 Interpretation of the exposure ages

The six exposure ages were obtained to determine the age of moraine stabilization and hence to provide insight into the time of the corresponding glacier advance which preceded moraine stabilization. Based on the topographical situation, we exclude by great certainty rock fall as the origin of boulder deposition for the various sample locations (Figure 2). Rather more, since the sampled boulders are located directly on the crest or the proximal side of the moraine, we assume that the boulders were transported by the glacier that formed the moraine. As can be deduced from numerous other palaeoclimatic records and knowledge of Alpine glacier advances during the early Holocene (Heiri et al. 2003, Magny et al. 2007, Samartin et al. 2012, Heiri et al. 2014), it can be concluded that the small Schwärzkar cirque glacier responded to a multi-decadal to a multi-centennial cooling phase persisting for a much shorter time period than the range of ages obtained through ^{36}Cl dating. Therefore, some ages may be either older or younger than the glacier advance, which formed the moraine. Ages that are too old would imply the inheritance of cosmogenic nuclides in a sampled boulder surface through pre-exposure. However, studies show that calculated ages preceding the true age of a landform are rare (Putkonen & Swanson 2003, Ivy-Ochs & Kober 2008). Conversely, ages that are too young would result from numerous post-depositional processes influencing the continual build-up of nuclides in the boulder surface, among which are spalling of a boulder, tilting and exhumation. Such disturbances are observed much more commonly (Hallet & Putkonen 1994, Heyman et al. 2011). Therefore, in compliance with Briner et al. (2005), we consider the obtained exposure ages to represent minimum ages meaning that the oldest ages (COB-2; 11.0±0.9 ka and 9.9±0.6 ka, COB-4), which are not significantly different from each other, are likely the most representative minimum ages for moraine stabilization. They have in common that they both stem directly from the moraine crest. Together they have a mean age of 10.4±0.8 ka. All other ages (9.1±0.5 ka, COB-3; 9.0±0.7 ka, COB-201; 8.9±0.5 ka, COB-202 and 8.2±0.5 ka, COB-203) are younger and come from central positions on the rock glacier like forms within the former glacier tongue area (Figure 4). These four ages cluster together forming a mean age of 8.8±0.5 ka, thus indicating either post glacial disturbances of nuclide buildup in the sampled rock surfaces or the possibility of continued boulder instability due to rock glacier deformation. The probability density functions of the sample ages are shown in Figure 5 showing the large age span throughout the early Holocene with both sample groups (i) from the moraine ridge and (ii) from the rock glacier surface on the proximal side of the moraine. The relict rock glaciers higher up, partially cutting the moraine discordantly and the hummocky deposits indicate that after the Schwärzkar glacier reached its terminal position and ice decay set in, some ice may have persisted under debris and sediment, supporting the formation of locally ice-rich discontinuous permafrost. Prolonged periods of possible periglacial creeping with interruptions in between, may have occurred in these elevations during several climate down-

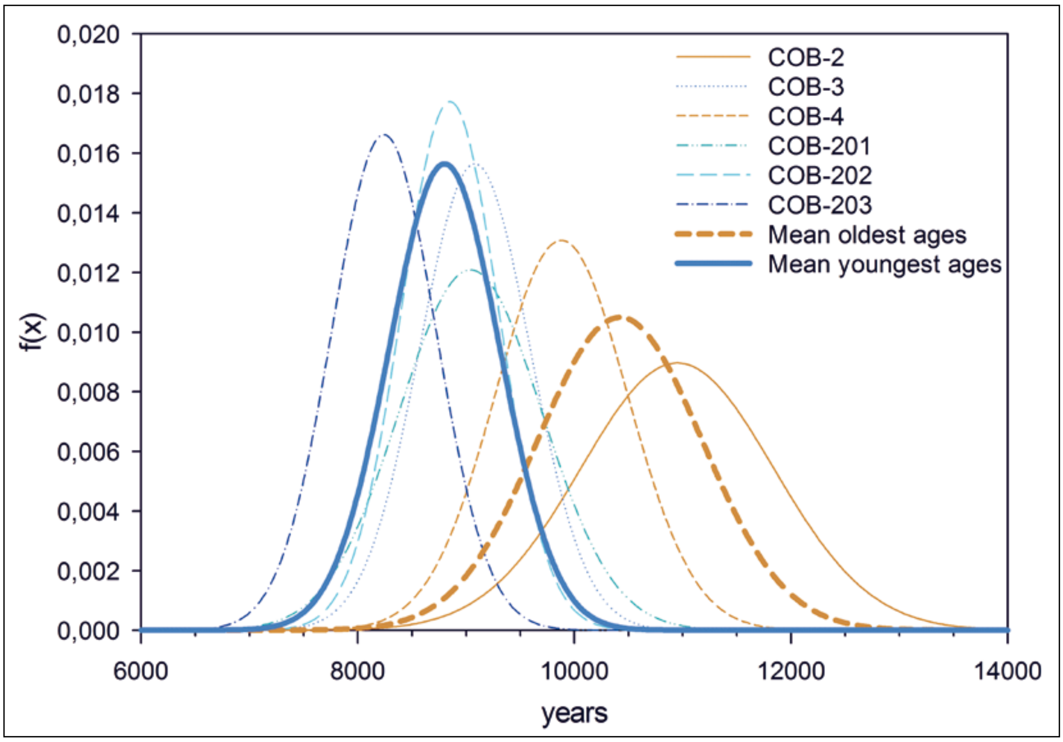

Fig.5: Probability density functions of the sample ages.

Abb. 5: Wahrscheinlichkeitsdichtefunktionen der Probenalter.

turns of the early Holocene, e.g. between ~10.1 and 10.6 ka (Schindelwig et al. 2011, Schimmelpfennig et al. 2014, Moran, Kerschner & Ivy-Ochs 2015), 9.2 ka (Fleitmann et al. 2008) and 8.2 ka (Nicolussi & Schlüchter 2012). Therefore, it is conceivable that final stabilization of the landforms constrained by the Schwärzkar moraine may not have set in until the beginning of the warm Holocene climate optimum (Joerin et al. 2008).

5.2 Climatic inferences

High precipitation sums in combination with reduced short-wave radiation in the well-shaded northern facing cirques of the Mieminger Range led to extraordinary low ELAs during the LIA in comparison to many other Alpine regions (Senarclens-Grancy 1938, Maisch 1999). Relative to the LIA, the glacier advance in the Schwärzkar showed a ΔELA of -120 m, or ~-70 to -90 m, if a significant influence of a debris cover is assumed. This is in agreement with evidence of other glacier advances in the Alps with moraine stabilization during the Preboreal period (Table 4). As these advances show similar ΔELAs in different regions of the Alps, we conclude that precipitation patterns were presumably similar to modern times (Moran et al. 2016), in contrast to the preceding Younger Dryas cold period, for which increased gradients between the humid northern and dry central Alps are assumed (Kerschner, Kaser & Sailer 2000). The relict rock glaciers up valley from the moraine system indicate one or several periods of cool and possibly somewhat drier climate conditions during and after the glacier recession. They may have begun to form contemporaneously to the initial melt back of the glacier in combination with the formation of dead ice under a thick debris cover and its preservation under permafrost conditions (Giardino & Vitek 1988, Berthing 2011).

5.3 Chronology

Considering the ^{36}Cl ages as minimum ages (Briner et al. 2005), we suggest that the Schwärzkar glacier advance occurred most likely after the Pleistocene-Holocene boundary, following the transition from the Younger Dryas cold period to the Preboreal. It is probably synchronous with glacier extents exhibiting practically identical ΔELAs of slightly more than -100 m in the western and central Alps that were dated to the early Holocene. Similar ΔELAs were also determined for the “Bockten” advance (Maisch 1981) and the “Kartell” (Fraedrich 1979, Maisch 1981, Ivy-Ochs et al. 2006) stadial. While the Bockten advanve is not dated, the Kartell stadial, however, seems to be of late Younger Dryas age. In the neighbouring Wetterstein Mountains, the Schwärzkar glacier likely correlates to the local “Brunntal” stadial associated on the basis of a pollen analysis of moraine-covered fossil soil with a Preboreal glacier advance clearly exceeding LIA positions (Hirtlreiter 1992). For the moraines of the “Brunntal” stadial, Hirtlreiter (1992) reports ΔELAs of -85 to -135 m, which is in line with the results for the Schwärzkar glacier. Hence, the Schwärzkar moraines may correspond to a Preboreal climatic deterioration, possibly the brief climatic downturn of the Preboreal Oscillation (~11.4 ka; Schwander et al 2000, Rasmussen et al. 2006). A correlation with a somewhat later cooling around ~10.5 ka (Tinner & Kaltenrieder 2005) cannot be excluded but seems to be less likely because of the quite large ΔELA. In any case, the investigations agree well with other palaeoclimatic records showing that the early Holocene was a period during which glaciers in the Alps to the west of Brenner pass still advanced beyond any positions reached subsequently during the late Holocene (Schindelwig et al. 2011, Schimmelpfennig et al. 2012, Schimmelpfennig et al. 2014, Moran, Kerschner & Ivy-Ochs 2015, Moran et al. 2016). Further to the east such a

Tab. 4: Exposure-dated early Holocene Alpine glacier advances. All ^{10}Be ages were calculated with the Northeast North American production rate (Balco et al. 2009), which has proven to yield suitable results for the Alpine region (Claude et al. 2014). Ages refer to moraine stabilization.

Tab. 4: Frühholozäne Gletschervorstöße im Alpenraum, deren Alter der Moränenstabilisierung mit der Expositionsdatierung bestimmt wurden. Alle ^{10}Be Alter wurden mit der nordost-nordamerikanischen Produktionsrate (Balco et al. 2009) berechnet, die für den Alpenraum angemessene Ergebnisse erzielt hat (Claude et al. 2014).

Glacier	Location	Age (ka)	Source
Kromer	Austria	10.1±1.0 to 10.6±1.4	Moran, Kerschner & Ivy-Ochs (2015)
Steingletscher II	Switzerland	10.4±0.4	Schimmelpfennig et al. (2014)
Belalp	Switzerland	10.6±2.2	Schindelwig et al. (2011)
Hinteres Bergle	Austria	10.9±0.8	Moran et al. (2016)
Steingletscher I	Switzerland	11.1±0.2	Schimmelpfennig et al. (2014)
Falgin	Italy	11.2±0.9	Moran et al. (2016)
Tsidjiore Nouve Glacier II	Switzerland	11.2±0.2	Schimmelpfennig et al. (2012)
Tsidjiore Nouve Glacier I	Switzerland	11.4±0.4	Schimmelpfennig et al. (2012)

set of glacier advances is missing, as has been shown by surface exposure dating of boulders and polished bedrock in the upper Rauris valley (Bichler et al. 2016). The reason for this discrepancy is not yet clear. It may either be due to a systematic error of unknown origin in the dating of the moraines and preceding glacier advances in the west or, more likely, may have been caused by differing climatic conditions.

The results also fit well into our present state of knowledge of the eastern Alpine moraine sequence (Ivy-Ochs et al. 2008) and may form the basis for considerations on a northern Alpine moraine chronology derived therefrom. The dated moraine system lies more than 1.5 km up valley from lateral moraines of an older oscillating glacier extending north of Seebensee and just reaching over the steep Seebenwände rock walls below which no end moraines were preserved. While Penck & Brückner (1901–1909) classified the moraines and similar moraines in the neighbouring cirques as "Gschnitz", Senarclens-Grancy (1938) argued that due to their position relative to the LIA moraines they must be younger and part of the "younger stadials" ("jungstadiale Gruppe"). The lateral moraine segments mark the margins of a glacier with an estimated ELA between 1900 and 1950 m a.s.l. and hence with a ΔELA from ~-350 to -400 m. These values agree well with those of numerous other large and well-preserved moraine systems in the vicinity (Hirtlreiter 1992, Kerschner 1993, Moran et al. 2016). They likely correspond to the multi-phased Egesen stadial that has been associated with the late Pleistocene Younger Dryas cold phase (12.9–11.7 ka; Rasmussen et al. 2006) in many parts of the Alps (Ivy-Ochs et al. 2009, and references therein). In comparable positions in the Northern Calcareous Alps in Tyrol, the ELA of possible Gschnitz stadial glaciers (~16.5–17 ka; Ivy-Ochs et al. 2006) is in the range of 1500–1700 m, depending on the position relative to the northern fringe of the Alps (Hirtlreiter 1992, Kerschner 1993 and unpublished data). Accordingly, more or less all of our research area would have been part of the accumulation area of the Gschnitz stadial glacier, which is in line with Senarclens-Grancy (1938).

6 Conclusions

The investigation of the Schwärzkar moraine system in the Mieminger Range provides evidence of a final glacier advance preceding the Little Ice Age glaciation of the cirque. The former glacier exceeded that of modern times significantly, while exhibiting a lowering of the equilibrium line altitude of -70 to -120 m. The numerical dating of boulders on the moraine shows that it was stabilized during the early Holocene period, with the mean of the oldest ages pointing to a minimum moraine stabilization age of around 10.4 ka, while the oldest age amounts to 11.0±0.9 ka. This agrees well with other dated moraines in the Alpine region west of Brenner pass indicating widespread Alpine glacier activity in the Preboreal period, perhaps in connection with the Preboreal Oscillation. Further boulders from hummocky deposits on the proximal side of the moraine show considerably younger ages with a mean age around 8.8±0.5 ka. These ages suggest that the final stabilization of boulders set in approximately 1 to 2 ka after moraine deposition. This may be the result of prolonged periglacial activity concomitantly with, or in various phases after glacier retreat in the well-shaded cirque. The chronostratigraphically younger relict rock glaciers located above the moraine system support the idea of prolonged periglacial activity following the glacier advance.

7 Acknowledgements

This study was made possible by the Austrian Science Foundation FWF that funded project P23601-N21. Furthermore we are grateful to the members of the Laboratory of Ion Beam Physics, ETH Zurich for their kind assistance in the laboratory and for carrying out the AMS measurements.

8 References

Alfimov, V. & Ivy-Ochs, S. (2009): How well do we understand production of ^{36}Cl in limestone and dolomite? – Quaternary Geochronology, 4: 462–474.

André, M.F. (2002): Rates of postglacial rock weathering on glacially scoured outcrops (Abisko-Riksgränsen Area, 68°N). – Geografiska Annaler, Series A, Physical Geography, 84: 139–150.

Balco, G., Stone, J.O., Lifton, N.A. & Dunai, T.J. (2008): A complete and easily accessible means of calculating surface exposure ages or erosion rates from ^{10}Be and ^{26}Al measurements. – Quaternary Geochronology, 3: 174–195.

Balco, G., Briner, J., Finkel, R.C., Rayburn, J.A., Ridge, J.C. & Schaefer, J.M. (2009): Regional beryllium-10 production rate calibration for lateglacial northeastern North America. – Quaternary Geochronology, 4: 93–107.

Becke, M. (1983): Zur Geologie des Mieminger Gebirges. – Geologische Paläontologische Mitteilungen Innsbruck, 12: 317–340.

Berthling, I. (2011): Beyond confusion: Rock glaciers as cryo-conditioned landforms. – Geomorphology, 131: 98–106.

Bichler, M., Reindl, M., Reitner, J.M., Drescher-Schneider, R., Wirsig, Ch., Christl, M., Hajdas, I. & Ivy-Ochs, S. (2016): Landslide deposits as stratigraphical markers for a sequence-based glacial stratigraphy: a case study of a Younger Dryas system in the Eastern Alps. – Boreas, 45: 537–551.

Björck, S., Rundgren, M., Ingolfsson, O. & Funder, S. (1997): The Preboreal oscillation around the Nordic Seas: terrestrial and lacustrine responses. – Journal of Quaternary Science, 12: 455–465.

Briner, J.P., Kaufman, D.S., Manley, W.F., Finkel, R.C. & Caffee, M.W. (2005): Cosmogenic exposure dating of late Pleistocene moraine stabilization in Alaska. – Geological Society of America Bulletin, 117: 1108–1120.

Carr, S.J., Lukas, S. & Mills, S.C. (2010): Glacier reconstruction and mass-balance modelling as a geomorphic and palaeoclimatic tool. – Earth Surface Processes and Landforms, 35: 1103–1115.

Christl, M., Vockenhuber, C., Kubik, P.W., Wacker, L., Lachner, J., Alfimov, V. & Synal, H.A. (2013): The ETH Zurich AMS facilities: Performance parameters and reference materials. – Nuclear Instruments and Methods in Physics Research Section B: Beam Interactions with Materials and Atoms, 294: 29–38.

Claude, A., Ivy-Ochs, S., Kober, F., Antognini, M., Salcher, B., Kubik, P.W. (2014): The Chironico landslide (Valle Leventina, southern Swiss Alps): age and evolution. – Swiss Journal of Geosciences, 107: 273–291.

Cossart, E., Fort, M., Bourlès, D., Braucher, R., Perrier, R. & Siame, L. (2012): Deglaciation pattern during the Lateglacial/Holocene transition in the southern French Alps. Chronological data and geographical reconstruction from the Clarée Valley (upper Durance catchment, southeastern France). – Palaeogeography, Palaeoclimatology, Palaeoecology, 315–316: 109–123.

Dunai, T.J. (2010): Cosmogenic nuclides. Principles, concepts and applications in the earth surface sciences. – 187 S.; Cambridge (Cambridge University Press).

Federici, P.R., Granger, D.E., Pappalardo, M., Ribolini, A., Spagnolo, M., Cyr, A.J. (2008): Exposure age dating and Equilibrium Line Altitude reconstruction of an Egesen moraine in the Maritime Alps, Italy. – Boreas, 37: 245–253.

Fleitmann, D., Mudelsee, M., Burns, S.J., Bradley, R.S., Kramers, J. & Matter, A. (2008): Evidence for a widespread climatic anomaly at around 9.2 ka before present. – Paleoceanography, 23 (1).

Frei, C. & Schmidli, J. (2006): Das Niederschlagsklima der Alpen: Wo sich Extreme nahe kommen. – Atmosphäre und Gebirge, 59: 61.

Geographie Innsbruck (2013): Tirol Atlas: Kartenset ‚Niederschlag': Mittlerer Jahresniederschlag 1961–1990. http://tirolatlas.uibk.ac.at/maps/thema/de/sheets/1168.pdf (accessed June 2016).

Giardino, J.R., & Vitek, J.D. (1988): The significance of rock glaciers in the glacial-periglacial landscape continuum. – Journal of Quaternary Science, 3: 97–103.

Gosse, J.C. & Phillips, F.M. (2001): Terrestrial in situ cosmogenic nuclides: theory and application. – Quaternary Science Reviews, 20: 1475–1560.

Gross, G. Kerschner, H. & Patzelt, G. (1977): Methodische Untersuchungen über die Schneegrenze in alpinen Gletschergebieten. – Zeitschrift für Gletscherkunde und Glazialgeologie, 7: 223–251.

Hallet, B. & Putkonen, J. (1994): Surface Dating of Dynamic Landforms: Young Boulders on Aging Moraines. – Science, 265: 937–940.

Heiri, O., Lotter, A.F., Hausmann, S. & Kienast, F. (2003): A chironomid-based Holocene summer air temperature reconstruction from the Swiss Alps. – The Holocene, 13: 477–484.

Heiri, O., Koinig, K.A., Spötl, C., Barrett, S., Brauer, A., Drescher-Schneider, R., Gaar, D., Ivy-Ochs, S., Kerschner, H., Luetscher, M., Moran, A., Nicolussi, K., Preusser, F., Schmidt, R., Schoeneich, P., Schwörer, C., Sprafke, T., Terhorst, B. & Tinner, W. (2014): Palaeoclimate records 60–8 ka in the Austrian and Swiss Alps and their forelands. – Quaternary Science Reviews, 106: 186–205.

Heyman, J., Stroeven, A.P., Harbor, J.M. & Caffee, M.W. (2011): Too young or too old: Evaluating cosmogenic exposure dating based on an analysis of compiled boulder exposure ages. – Earth and Planetary Science Letters, 302: 71–80.

Hirtlreiter, G. (1992): Spät- und postglaziale Gletscherschwankungen im Wettersteingebirge und seiner Umgebung. – Dissertation, University of Munich. – 154 S.; Munich.

Ivy-Ochs, S. & Kober, F. (2008): Surface exposure dating with cosmogenic nuclides. – Eiszeitalter & Gegenwart, 57: 179–209.

Ivy-Ochs, S. & Schaller, M. (2009): Examining Processes and Rates of Landscape Change with Cosmogenic Radionuclides. – In: Klaus, F. (Ed.): Radioactivity in the Environment, 16: 231–294.

Ivy-Ochs, S., Synal, H. A., Roth, C. & Schaller, M. (2004): Initial results from isotope dilution for Cl and ^{36}Cl measurements at the PSI/ETH Zurich AMS facility. – Nuclear Instruments and Methods in Physics Research Section B: Beam Interactions with Materials and Atoms, 223–224: 623–627.

Ivy-Ochs, S., Kerschner, H., Reuther, A., Maisch, M., Sailer, R., Schaefer, J., Kubik, P.W., Synal, H., Schlüchter, C. (2006): The timing of glacier advances in the northern European Alps based on surface exposure dating with cosmogenic ^{10}Be, ^{26}Al, ^{36}Cl, and ^{21}Ne. – In: Siame, L.L., Bourlès, D.L. & Brown, E.T. (Eds.): In Situ-Produced Cosmogenic Nuclides and Quantification of Geological Processes. – Geological Society of America Special Paper: 43–60.

Ivy-Ochs, S., Kerschner, H., Reuther, A., Preusser, F., Heine, K., Maisch, M., Kubik, P.W. & Schlüchter, C. (2008): Chronology of the last glacial cycle in the European Alps. – Journal of Quaternary Science, 23: 559–573.

Ivy-Ochs, S., Kerschner, H., Maisch, M., Christl, M., Kubik, P.W. & Schlüchter, C. (2009): Latest Pleistocene and Holocene glacier variations in the European Alps. – Quaternary Science Reviews, 28: 2137–2149.

Joerin, U.E., Nicolussi, K., Fischer, A., Stocker, T.F. & Schlüchter, C. (2008): Holocene optimum events inferred from subglacial sediments at Tschierva Glacier, Eastern Swiss Alps. – Quaternary Science Reviews, 27: 337–350.

Jóhannesson, T., Raymond, C.F. & Waddington, E.D. (1989): A simple method for determining the response time of glaciers. – In: Oerlemans, J. (Ed.): Glacier fluctuations and climate change. – Proceedings of the symposium on glacier fluctuations and climatic change. 243–352; Amsterdam (Kluwer Academic Publishers).

Keller, O. (1988): Ältere spätwürmzeitliche Gletschervorstösse und Zerfall des Eisstromnetzes in den nördlichen Rhein-Alpen (Weissbad-Stadium/Bühl-Stadium). – Band A. Physische Geographie, 27. Institute of Geography, University of Zurich Zurich.

Kelly, M. A., Kubik, P. W., Von Blanckenburg, F. & Schlüchter, C. (2004): Surface exposure dating of the Great Aletsch Glacier Egesen moraine system, western Swiss Alps, using the cosmogenic nuclide ^{10}Be. – Journal of Quaternary Science, 19: 431–441.

Kerschner, H. (1993): Späteiszeitliche Gletscherstände im südlichen Karwendel bei Innsbruck, Tirol. – In: Petermüller-Strobl, M. & Stötter, J. (Hrsg.): Der Geograph im Hochgebirge. Beiträge zu Theorie und Praxis geographischer Forschung (Festschrift für Helmut Heuberger). – Innsbrucker Geographische Studien, 20: 47–55.

Kerschner, H., Kaser, G. & Sailer, R. (2000): Alpine Younger Dryas glaciers as palaeo-precipitation gauges. – Annals of Glaciology, 31: 80–84.

Kirkbride, M.P., Mitchell, W A. & Barnes, M. (2015): Reconstruction and Regional Significance of the Coire Breac Palaeoglacier, Glen Esk, Eastern Grampian Highlands, Scotland. – Geografiska Annaler, Series A, Physical Geography, 97: 563–577.

Lal, D. (1991): Cosmic ray labeling of erosion surfaces: in situ nuclide production rates and erosion models. – Earth and Planetary Science Letters, 104: 424–439.

Magny, M., Vannière, B., de Beaulieu, J.-L., Bégeot, C., Heiri, O., Millet, L., Peyron, O. & Walter-Simonnet, A.-V. (2007). Early-Holocene climatic oscillations recorded by lake-level fluctuations in west-central Europe and in central Italy. – Quaternary Science Reviews, 26: 1951–1964.

Maisch, M. (1981): Glazialmorphologische und gletschergeschichtliche Untersuchungen im Gebiet zwischen Landwasser- und Albulatal (Kt. Graubünden, Schweiz). – 215 S.; Zurich (Universität Zürich).

Maisch. M. (1999): Die Gletscher der Schweizer Alpen: Gletscherhochstand 1850, aktuelle Vergletscherung, Gletscherschwund-Szenarien. – Projektschlussbericht im Rahmen des Nationalen Forschungsprogrammes „Klimaänderungen und Naturkatastrophen" – NFP 31. 373 S.; Zürich (Vdf Hochschulverlag).

Maisch, M. (2000): The longterm signal of climate change in the Swiss Alps: glacier retreat since the end of the Little Ice Age and future ice decay scenarios. – Geografia Fisica e Dinamica Quaternaria, 23: 139–151.

Miller, H. (1962): Der Bau des westlichen Wettersteingebirges. – Zeitschrift der deutschen Geologischen Gesellschaft, 113: 409–425.

Moran, A.P., Kerschner, H. & Ivy-Ochs, S. (2015): Redating the moraines in the Kromer Valley (Silvretta Mountains). – New evidence for an early Holocene glacier advance. – The Holocene, 26: 655–664.

Moran, A.P., Ivy-Ochs, S., Schuh, M., Christl, M. & Kerschner, H. (2016): Evidence of central Alpine glacier advances during the Younger Dryas–early Holocene transition period. – Boreas, 45: 398–410.

Moran, A. P., Ivy-Ochs, S., Vockenhuber, Ch. & Kerschner, H. (2016): Rock glacier development in the Northern Calcareous Alps at the Pleistocene-Holocene Boundary. – Geomorphology, 273: 178–188.

Nicolussi, K. & Schlüchter, C. (2012): The 8.2 ka event – Calendar-dated glacier response in the Alps. – Geology, 40: 819–822.

Penck, A. & Brückner, E. (1901–1909): Die Alpen im Eiszeitalter. 1149 S.; Leipzig (Tauchnitz).

Putkonen, J. & Swanson, T. (2003): Accuracy of cosmogenic ages for moraines. – Quaternary Research, 59: 255–261.

Rasmussen, S.O., Andersen, K.K., Svensson, A.M., Steffensen, J.P., Vinther, B.M., Clausen, H.B., Siggaard-Andersen, M.L., Johnsen, S.J., Larsen, L.B., Dahl-Jensen, D., Bigler, M., Röthlisberger, R., Fischer, H., Goto-Azuma, K., Hansson, M.E. & Ruth, U. (2006): A new Greenland ice core chronology for the last glacial termination. – Journal of Geophysical Research, 111 (D6).

Reber, R., Akçar, N., Ivy-Ochs, S., Tikhomirov, D., Burkhalter, R., Zahno, C., Lüthold, A., Kubik, P.W., Vockenhuber, C. & Schlüchter, C. (2014): Timing of retreat of the Reuss Glacier (Switzerland) at the end of the Last Glacial Maximum. – Swiss Journal of Geosciences, 107: 293–307.

Samartin, S., Heiri, O., Vescovi, E., Brooks, S.J. & Tinner, W. (2012): Lateglacial and early Holocene summer temperatures in the southern Swiss Alps reconstructed using fossil chironomids. – Journal of Quaternary Science, 27: 279–289.

Schimmelpfennig, I., Schaefer, J. M., Akçar, N., Ivy-Ochs, S., Finkel, R. C. & Schlüchter, C. (2012): Holocene glacier culminations in the Western Alps and their hemispheric relevance. – Geology, 40: 891–894.

Schimmelpfennig, I., Schaefer, J. M., Akçar, N., Koffman, T., Ivy-Ochs, S., Schwartz, R., Finkel, R. C., Zimmerman, S. & Schlüchter, C. (2014): A chronology of Holocene and Little Ice Age glacier culminations of the Steingletscher, Central Alps, Switzerland, based on high-sensitivity beryllium-10 moraine dating. – Earth and Planetary Science Letters, 393: 220–230.

Schindelwig, I., Akçar, N., Kubik, P.W. & Schlüchter, C. (2011): Lateglacial and early Holocene dynamics of adjacent valley glaciers in the Western Swiss Alps. – Journal of Quaternary Science 27: 114–124.

Schoeneich, P. (1998): Le retrait glaciaire dans les vallées des Ormonts, de l'Hongrin et de l'Etivaz (Préalps vaudoises). – 483 S.; Lausanne (Institut de Géographie, Université de Lausanne).

Senarclens-Grancy, W.v. (1938): Stadiale Moränen in der Mieminger Kette und im Wetterstein. – Jahrbuch der Geologischen Bundesanstalt, 88: 1–12.

Stone, J.O. (2000): Air pressure and cosmogenic isotope production. – Journal of Geophysical Research: Solid Earth, 105: 23753–23759.

Stone, J.O., Allan, G.L., Fifield, L.K. & Cresswell, R.G. (1996): Cosmogenic chlorine-36 from calcium spallation. – Geochimica et Cosmochimica Acta, 60: 679–692.

Tinner, W. & Kaltenrieder, P. (2005): Rapid responses of high-mountain vegetation to early Holocene environmental changes in the Swiss Alps. – Journal of Ecology, 93: 936–947.

Zreda, M.G., Phillips, F.M. & Elmore, D. (1994): Cosmogenic ^{36}Cl accumulation in unstable landforms. Two simulations and measurements on eroding moraines. – Water Resources Research, 30: 3127–3136.